

Grain Boundary Character and Microstructural Evolution During Hot Deformation of a High Nb Containing TiAl Alloy

Zhao Ruifeng, Zhou Huan, Zhang Tiebang, Kou Hongchao, Li Jinshan

State Key Laboratory of Solidification Processing, Northwestern Polytechnical University, Xi'an 710072, China

Abstract: Grain boundary character and microstructural evolution during hot deformation of a high Nb-containing TiAl alloy with the composition of Ti-45Al-8.5Nb-(W,B,Y) was investigated. The plasma arc-melted alloy exhibits nearly lamellar microstructures with $\beta/\text{B2}$ phase precipitates along colony boundaries. The retained $\beta/\text{B2}$ phase rich in Ti, Nb and W and poor in Al is formed by the $\beta \rightarrow \alpha$ transformation during nonequilibrium solidification. This $\beta/\text{B2}$ precipitation is caused by the high cooling rate, low atom diffusion rate of β stabilizers and different partition coefficients of the elements. B and Y elements exist mainly as borides and Y_2O_3 , respectively. The morphology, size, composition and stability of $\beta/\text{B2}$ phase are determined by hot deformation. The high temperature and press enhance the elements diffusion, and thus the variation of the composition of $\beta/\text{B2}$ phase in deformed samples is obviously observed. When the samples are deformed in $(\alpha + \gamma)$ phase region, the transformation $\beta/\text{B2} \rightarrow \alpha_2$ takes place. Considering the different crystal structures of $\beta/\text{B2}$ and α_2 phases, there is a tendency for $\beta/\text{B2}$ phase to transform to a more closed packed structure of α_2 during deformation. The $\beta/\text{B2} \rightarrow \alpha_2$ transformation is promoted by the hot deformation.

Key words: TiAl; grain character; microstructural evolution; microsegregation; hot deformation

Due to their high specific yield strength, good creep properties and high oxidation resistance at elevated temperature, TiAl-based alloys are promising light-weight structural materials for high-temperature applications in automobile, aerospace and nuclear industries^[1-3]. However, the poor formability and low ductility at room temperature are major problems which restrict their practical applications of TiAl alloys^[4,5]. To achieve a good balance between room temperature ductility and high temperature properties, great efforts have been devoted, including element alloying, heat treatment and hot working in this field^[6-8].

At present, the addition of Nb, W and other β -stabilizing elements is an effective way to improve properties of TiAl-based alloys^[9]. As heavy refractory metals, Nb and W shift the Ti-Al phase diagram to a higher temperature^[1]. Accordingly, the liquidus temperature increases and the service range of these materials can be extended to higher temperature. In recent years, high Nb containing TiAl alloys have attracted much attention because of their excellent high

temperature strength and oxidation resistance^[10]. In order to further control microstructures and keep balance properties of the alloys, some other micro-alloying elements, such as B and Y, can be added. Micro-alloying with B and Y can refine the microstructure effectively, which is conducive to improving strength-ductility balance as well as contributing to hot deformability of TiAl alloys^[11-14]. Unfortunately, the different melting point, density and diffusion capacity of the elements in high Nb containing TiAl alloys lead to significant segregation in the alloy produced by conventional ingot metallurgy^[15]. Al-segregation and β phase segregation (β -segregation and α -segregation) are always found in the as-cast alloys with different ingot production methods and compositions^[15-18]. During non-equilibrium solidification, some elements which have different solubility in each phase are easy to be pushed to grain boundaries with the phase transformation and grain boundary migration to result in microsegregation, which inevitably affect the combination of the adjacent grains. At the same time, the added β -stabilizing

Received date: October 25, 2017

Foundation item: National Basic Research Program of China (2011CB605503); "111" Project (B08040)

Corresponding author: Zhang Tiebang, Ph. D., Professor, Northwestern Polytechnical University, Xi'an 710072, P. R. China, Tel: 0086-29-88491764, E-mail: tiebangzhang@nwpu.edu.cn

Copyright © 2018, Northwest Institute for Nonferrous Metal Research. Published by Elsevier BV. All rights reserved.

elements always change the solidification path and microstructure^[1,9], which can also make a contribution to grain boundary segregation in high Nb containing TiAl alloys.

A large amount of β phase at grain boundaries form due to chemical segregation, especially β -stabilizing elements, which significantly improves the hot deformability^[19,20]. The disordered β phase is a ductile phase at elevated temperatures^[19]. Besides, the body-centered cubic β phase with sufficient number of independent slip systems is considered to be softer than the matrix. However, B2 is the ordered structure of β phase at low temperatures. β /B2 phase can be the site where microcracks can form and it does harm to the room temperature ductility and creep properties^[21-23]. It means that a certain volume fraction of disordered β phase is necessary to be kept during hot-forming operations, but the β /B2 phase should be eliminated before the service of the alloys. It is found that the amount of remained β /B2 can be reduced by controlling heat treatments. Clemens et al.^[19,24] have shown that the volume fraction of the β /B2 phase reaches a minimum around the α -transus temperature after heat treatment. And similar results have been obtained by Huang et al.^[22]. In addition, it has been also reported by Zhang et al.^[25] that the β /B2 phase cannot be removed completely only by heat treatments, but it can be almost eliminated with applying external pressure. After forged in the $(\alpha + \gamma)$ phase region, homogenous duplex (DP) microstructure without β /B2 phase can be obtained^[8,16]. However, little attention has been paid to the details of β /B2 phase in the change of composition, structure and phase transformation during hot deformation.

The present study aims at investigating the characteristics of microsegregation in the high-Nb containing TiAl alloy and the change of β /B2 phase in detail during hot deformation. In this work, the type, distribution and morphology of microsegregation in a high Nb-containing TiAl ingot are described. Then the changes of composition, structure, distribution of β /B2 phase during high temperature compression tests are investigated to illustrate grain boundary character and microstructural evolution during hot deformation. In addition, grain boundary segregation behavior of the high Nb-containing TiAl alloy and the evolution of β /B2 phase during hot deformation are also discussed.

1 Experiment

The investigated alloy with the nominal composition of Ti-45Al-8.5Nb-(W,B,Y) (at%) was prepared by plasma arc melting process by Bao Steel Co., Ltd. Cylindrical compression specimens with a diameter of 8 mm and a height of 12 mm were cut from the ingot by electric-discharge machining. Hot-compression tests were conducted on a Gleeble-3500 machine at temperatures of 850, 1000, 1100, 1200 °C at strain rates of 10^{-1} , 10^{-2} and 10^{-3} s⁻¹. To minimize the friction, tantalum foils were employed as lubricant during isothermal compression. Each sample was heated at a rate of 10 °C/s and stabilized for 5

min at the target temperature. All the samples were deformed to engineering strain of 60%. To preserve the deformed microstructure, samples were water quenched to room temperature immediately once the compression tests finished.

The deformation specimens were sectioned parallel to the compression axis for microstructural observation. The microstructures were characterized by optical microscopy (OM), scanning electron microscopy (SEM) in back-scattered electron (BSE) mode and energy dispersive spectroscopy (EDS). And the samples for microstructural observation were mechanically polished and then etched in a Kroll's reagent. Compositions of the various microstructural constituents was determined by electron probe microanalysis (EPMA) and X-ray mapping. Phase constituent and crystal structure were analyzed by X-ray diffraction (XRD) using Cu K α radiation. For transmission electron microscopy (TEM) observation, thin TEM foils were prepared by mechanical polishing and ion milling. TEM observations were undertaken on a Tecnai G2 F30 transmission electron microscope working at 300 kV.

2 Results and Discussion

2.1 Microstructure and microsegregation

Microstructure of Ti-45Al-8.5Nb-(W,B,Y) alloy in as-cast condition is shown in Fig. 1a. The alloy mainly exhibits a uniform near lamellar (NL) structure consisting of lamellar colonies and some equiaxed grains at colony boundaries. The average colony size is ~120 μ m. The X-ray diffraction pattern is shown in Fig. 1b indicates the presence of γ , α_2 and β /B2 phases in the as-cast alloy. Additionally, the β /B2-feature

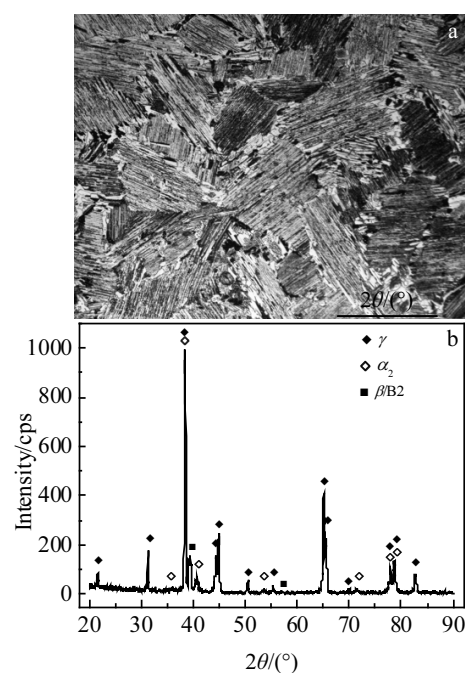


Fig.1 Optical microstructure (a) and XRD pattern (b) of as-cast Ti-45Al-8.5Nb-(W, B, Y) alloy

diffraction peak is prominent, which implies a considerable amount of $\beta/\text{B2}$ phase. This could be attributed to the addition of β -stabilizing elements and non-equilibrium solidification during the ingot preparation.

Fig.2 shows microstructure of the as-cast experimental alloy. BSE observation reveals that a white-contrast network is distributed throughout the matrix of the alloy. A part of the network exhibiting a faint outline is located at the lamellar matrix as indicated by arrow 3 in Fig.2a. EPMA analysis indicates that this region is enriched in Nb and W (Table 1). It is caused by segregation of Nb and W to dendrite cores during solidification^[17,18]. The white irregular-shaped block at colony boundaries and triple junctions is $\beta/\text{B2}$ phase which is confirmed by EPMA analysis (Table 1) and X-ray diffraction spectrum in Fig. 1b. As can be seen in Fig.2b, the $\beta/\text{B2}$ phase is occasionally intersected by small γ grains. This phenomenon originates from the discontinuous reaction $\beta \rightarrow \beta + \gamma$ during the cooling process^[26]. The EDS element liner scanning is shown in Fig.2d and composition analysis in Table 1 indicates that the $\beta/\text{B2}$ phase at boundaries (β -segregation) is rich in Ti, Nb and W but poor in Al. The observations suggest that the lamellar colonies, which come from prior α grains, contain a lower content of β -phase stabilisers (Nb and W). The volume fraction of the $\beta/\text{B2}$ phase is about 8%. The β -segregation lies in a size range 10~30 μm . The compositions at different positions in Fig.2 are summarized in Table 1.

Except for the main microsegregation of β phase, B-segregation and Y-segregation are observed as shown in the inset of Fig.2b and exist as borides and Y_2O_3 , respectively. The borides in the form of particle or rod are distributed within the colonies or colony boundaries. It is well known that borides exist in different morphologies and crystal structures in TiAl alloys, which is related to the boron content and solidification process^[27]. Yttrium oxide particles with bright contrast are mainly located at the boundaries, and the composition ratio of Y to O in the yttrium oxide particle is close to 2:3. The existence rate of O atom in the matrix is reduced by Y intrinsic oxidation. The volume fraction of Y_2O_3 is considerably low considering the content of Y is only 0.02 at%. It suggests that the solubility of Y is rather low in high Nb containing TiAl alloys. The reason for the absence of the borides and Y_2O_3 phase in XRD spectrum is that they are both too rare to be detected.

2.2 Microstructure evolution during hot deformation

Fig.3 shows SEM micrographs of the alloy deformed to 60% engineering strain under different conditions. For the samples deformed at 850 $^{\circ}\text{C}$ and 0.01 s^{-1} (Fig.3a), the $\beta/\text{B2}$ phase is elongated along the direction perpendicular to the compression axis. The bending lamellas in the unrecrystallized microstructures can be observed. Small cavities can be found between borides and the matrix as marked by arrows in the inset of Fig.3a. At the same time, rod-shaped borides are broken down

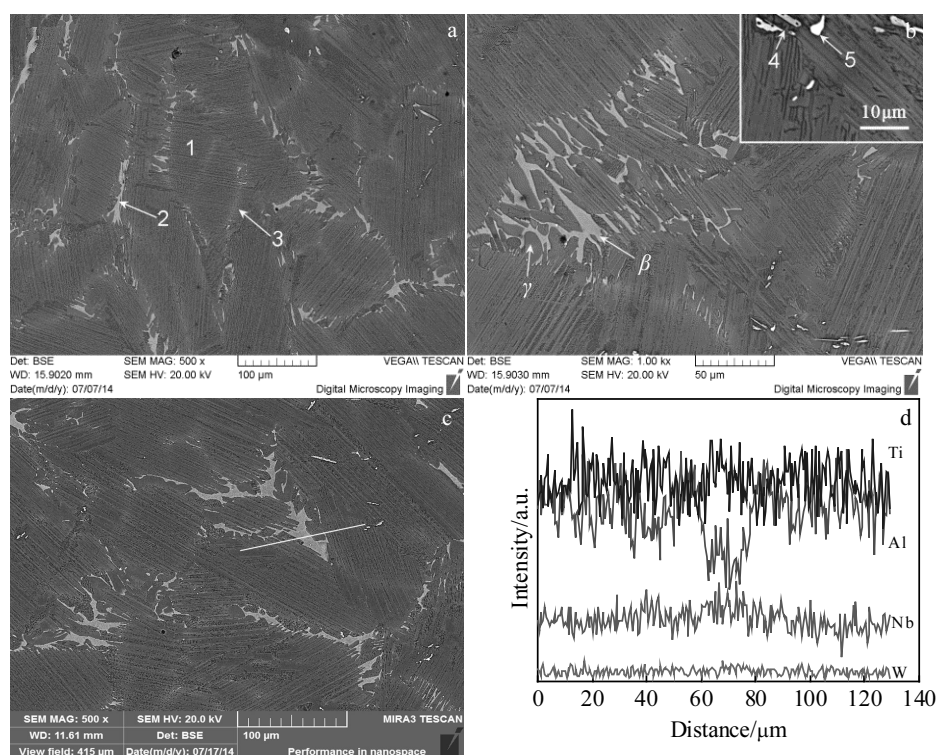


Fig.2 Microsegregation in the as-cast Ti-45Al-8.5Nb-(W, B, Y) alloy: (a) β phase segregation at grain boundaries and Nb, W enriched region; (b) boride and yttrium oxide segregation; (c, d) element liner scanning across $\beta/\text{B2}$ phase

Table 1 EPMA analysis of marked position 1~5 in Fig.2

Position	Ti	Al	Nb	W	B	Y	O
1 (lamellar colony) in Fig. 2a	47.40	44.72	7.70	0.18	-	-	-
2 (β phase) in Fig. 2a	54.33	34.48	10.70	0.49	-	-	-
3 (Nb and W enriched region) in Fig. 2a	49.08	42.02	8.56	0.34	-	-	-
4 (Y_2O_3) in Fig. 2b	7.85	8.14	-	-	-	33.02	50.99
5 (boride) in Fig. 2b	21.93	5.56	5.83	0.34	66.34	-	-

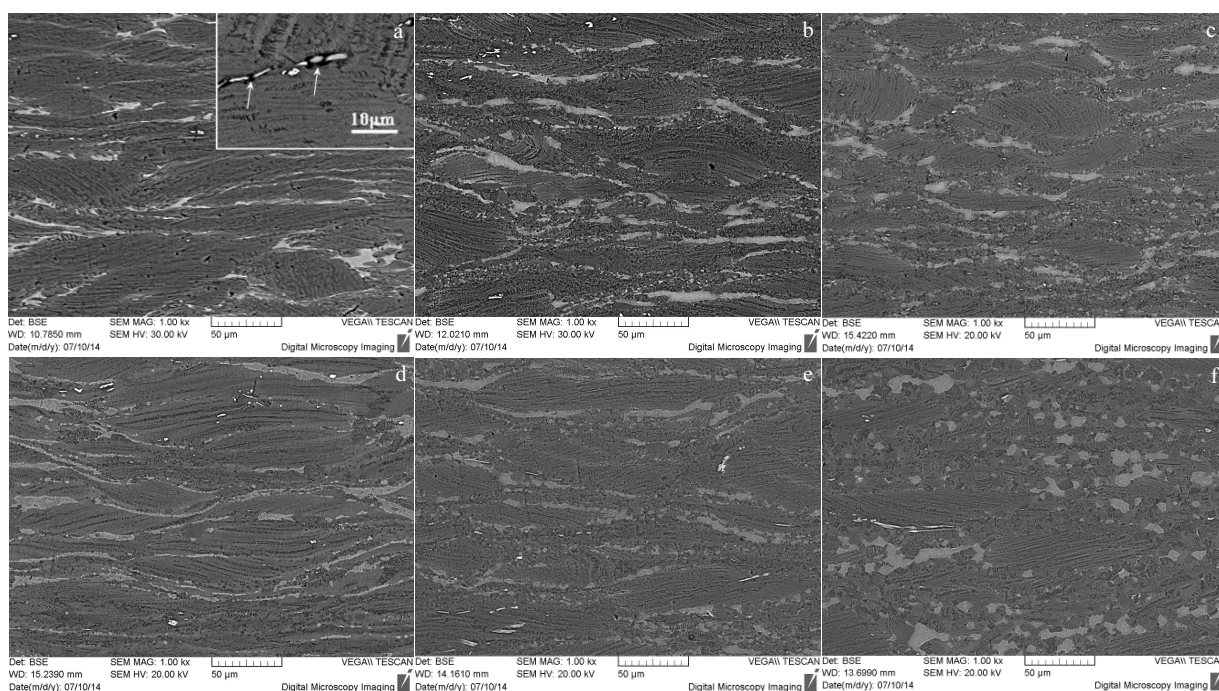


Fig.3 BSE images of the Ti-45Al-8.5Nb-(W,B,Y) alloy deformed with engineering strain of 60% under different conditions: (a) 850 °C/0.01 s⁻¹, (b) 1000 °C/0.01 s⁻¹, (c) 1100 °C/0.01 s⁻¹, (d) 1200 °C/0.1 s⁻¹, (e) 1200 °C/0.01 s⁻¹, and (f) 1200 °C/0.001 s⁻¹

into smaller sized ones in deformed samples. Small cavities are considered to be caused by stress concentration, which can also be observed in tensile samples^[28]. The borides are brittle, which are hard to deform compared with the matrix. At 1000 °C, the $\beta/B2$ phase is partially broken down into fine equiaxed particles as can be seen in Fig.3b. Dynamically recrystallized grains appear at grain boundaries area and the cavities between borides and the matrix are not observed. This indicates that the soft β phase at high temperatures accumulates sufficient strain, and the grain boundary β phase is the preferential place for dynamic recrystallization (DRX). The work of Liu et al.^[29] indicates that DRX can be an important softening mechanism in the as-cast high Nb containing TiAl alloys. It means that the soft β phase and recrystallized grains at grain boundaries facilitate the strain partitioning between lamellar colonies. Consequently, stress concentration in the matrix can be partially relieved, which is beneficial to avoiding the appearance of cavities at the

matrix/boride interfaces. The fraction of broken $\beta/B2$ particles and recrystallized grains increases with deformation temperature up to 1100 and 1200 °C as shown in Fig.3c and Fig.3e. When deformed at 1200 °C within the ($\alpha + \gamma$) phase field region (Fig.3d~3f), the decreasing of strain rate causes the change of $\beta/B2$ grains from elongated shapes to spheroidized ones. The same behavior of the $\beta/B2$ phase can be observed after deformed at higher temperatures^[30]. And the fraction of residual lamellar colonies decreases with decreasing strain rate. At the lowest strain rate of 0.001 s⁻¹, the $\beta/B2$ phase is almost fully spheroidized or equiaxed, as shown in Fig.3f. The average grain size of the $\beta/B2$ phase lies between 5 and 10 μm . It indicates that the $\beta/B2$ phase in deformed samples exhibits smaller size comparing with that of the as-cast alloy.

The microstructure details of the $\beta/B2$ phase in the sample deformed at 1100 °C and 0.01 s⁻¹ are revealed in Fig.4a. It can be clearly seen that the $\beta/B2$ phase located at the colony

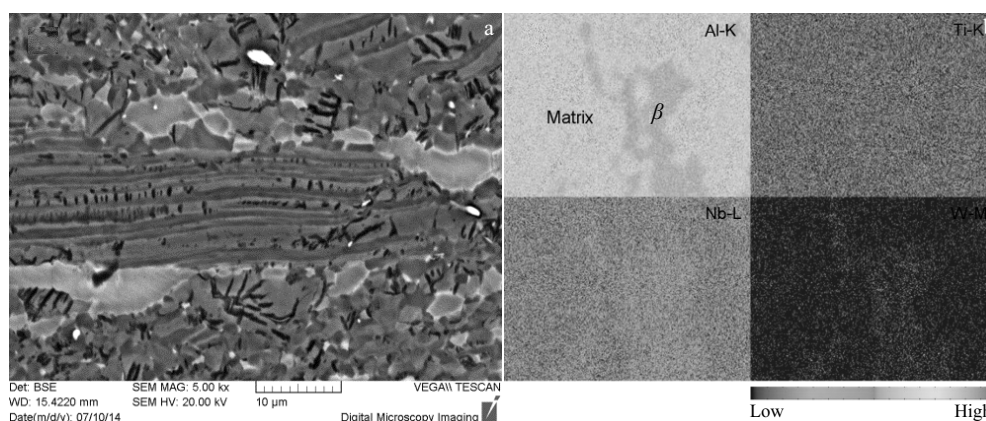


Fig.4 Microstructures after deformed at 1100 °C with strain rate of 0.01 s⁻¹: (a) BSE image showing β /B2 phase, (b) elemental EPMA-maps of Al, Ti, Nb and W from an analyzed section of 40 $\mu\text{m} \times 30 \mu\text{m}$ including β /B2 phase and the matrix

boundary is surrounded by recrystallized grains. A part of the β /B2 phase is broken down into small sized ones. SEM image in BSE mode presents that the interface between β /B2 phase and the matrix exhibits a bright contrast, which is considered to be caused by the diffusion of refractory metal elements, including Nb and W. EPMA analysis shows that the β /B2 phase has the average composition of 51.84Ti, 38.91Al, 8.89Nb and 0.36W (at%) in this condition. Compared with the as-cast condition, Nb and W contents in the β /B2 phase tend to decrease while the Al-content increases. As is well known, the diffusion rate is always governed by increasing temperature. Additionally, applying external press is also believed to enhance the diffusion of elements during hot compression due to the introduced defects. After deformation at 1100 °C with strain rate of 0.01 s⁻¹, the elemental distributions of Al, Ti, Nb and W are shown in Fig.4b. The β /B2 phase preserves a lower Al-content compared with that of the adjacent matrix. Nb and W contents in the β /B2 phase are still a little higher than those in the adjacent matrix.

The variation of unit cell volume for β /B2 phase with increasing deformation temperature is illustrated in Fig.5 (taking the unit cell volume of β /B2 phase in the deformed condition of 850 °C/0.01 s⁻¹ as the baseline). The unit cell volume of β /B2 phase slightly decreases with temperature from 850 °C up to 1100 °C. At 1200 °C, a slight increase in unit cell volume of β /B2 phase is related to composition change and phase transformation of β /B2 phase. The radius of Nb atoms is larger than that of Ti atoms, and the radius of Ti atoms is larger than that of Al atoms. Thus, the variation of the composition of β /B2 phase is responsible for the decrease of the unit cell volume. But when the temperature is raised to 1200 °C within the ($\alpha + \gamma$) phase field region, the lattice distortion induced by compressive stress can be partially relieved by phase transformation of β /B2 phase. And this can

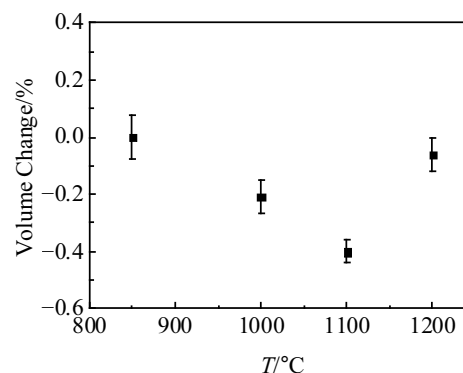


Fig.5 Variation of unit cell volume for β /B2 phase with increasing temperature of the alloy deformed with strain rate of 0.01 s⁻¹ and strain of 60% (taking the unit cell volume of β /B2 phase in the deformed condition of 850 °C/0.01 s⁻¹ as the baseline)

be the reason for the slight increase in unit cell volume of β /B2 phase at 1200 °C.

A more detailed observation of the β /B2 phase distributing in microstructures deformed at 1200 °C is given by SEM investigations as shown in Fig.6. The microstructures consist of residual lamellar colonies, β /B2 grains (white contrast), α_2 grains (grey contrast) and γ grains (dark contrast). In comparison to the as-cast alloy, significant α_2 grains are observed in the deformed microstructures. Generally, DRX proceeds preferentially in grain boundary β phase^[31]. When deformed in the ($\alpha + \gamma$) phase region, α and γ phases form mainly by DRX. The transformation of α phase into ($\alpha_2 + \gamma$) lamellae is suppressed by the high cooling rate. The β /B2 phase is surrounded by recrystallized grains in the microstructures deformed at different strain rates (Fig.6a, 6b). It is necessary to note that some β /B2 grains are entirely surrounded

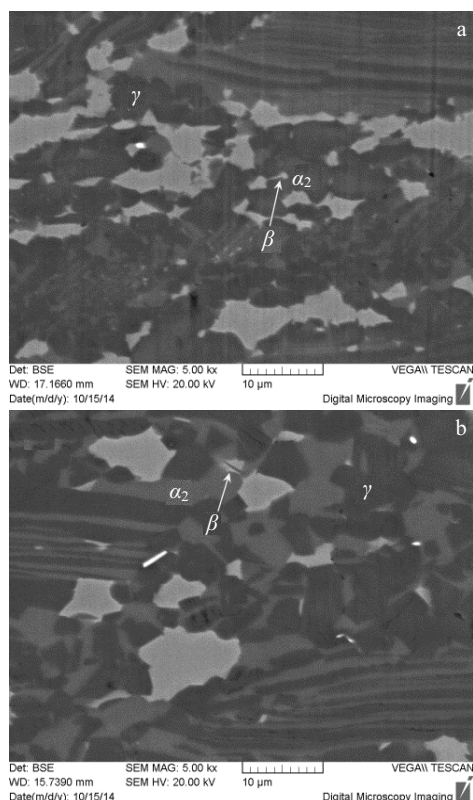


Fig.6 BSE images showing the distribution of β /B2 phase after deformed at 1200 °C with strain rate of 0.01 s⁻¹ (a) and 0.001 s⁻¹ (b)

by α_2 phase. This implies that the β /B2 phase is consumed by neighboring α_2 grains via β/α interface migration. According to the EPMA results, the β /B2 phase has the average composition (at%) of 49.84Ti, 41.05Al, 8.80Nb and 0.31W in the microstructure deformed at 1200 °C and 0.01 s⁻¹. The decrease of Nb and W contents in the β /B2 phase promotes the decomposition of metastable β phase.

TEM images and SAED patterns of deformed microstructure at 1200 °C and 0.001 s⁻¹ are shown in Fig.7. The bright-field TEM image in Fig.7a reveals the formation of thin secondary α_2 lath within the β /B2 grain. The phase with block morphology in the center of the TEM image as shown in Fig. 7a is confirmed to be β /B2 by SAED pattern in Fig.7b. Fig.7c shows the high-resolution image of the secondary phase in the β /B2 grain. The thin secondary lath is confirmed to be α_2 phase by the fast Fourier transform (FFT) image, as shown in the upper left inset in Fig.7c. And the interplanar spacing of $\{002\}_{\alpha_2}$ and $\{200\}_{\alpha_2}$ are measured as 0.2322 and 0.2501 nm, respectively. As seen from the upper right inset achieved by FFT/IFFT transformation in Fig.7c, the marked section of the center area is enlarged to show the lattice distortion in the thin secondary α_2 lath. The β /B2 phase can decompose into thin secondary α_2 lath through phase transformation β /B2 $\rightarrow\alpha_2$.

Diffraction pattern in Fig.7d indicates that the surrounding phase of the β /B2 grain is α_2 . A higher magnification of the interface between β grain and surrounding α_2 is shown in Fig.7e. A small amount of B2 particles (marked by arrow) pin the original location of the interface during the transformation, which indicates that the β /B2 grain can be consumed by surrounding α_2 .

3 Discussion

3.1 Origin of β phase segregation at grain boundaries

The segregation of Nb is significant in high Nb containing TiAl alloys, although the high temperature performance of TiAl-based alloys is significantly improved by Nb addition. The as-cast Ti-45Al-8.5Nb-(W,B,Y) alloy exhibits nearly lamellar microstructures, consisting of lamellar colonies and mixtures of β /B2 and γ grains along colony boundaries as shown in Fig.2. It is well known that the solidification pathway of TiAl-based alloys is closely related to the composition, i.e. Al-content and β -stabilizers addition^[1,19]. With high Nb addition, the β phase field extends to lower temperatures and higher Al concentration, while α phase field is contracted^[15]. The microstructure of the as-cast alloy shows the evidence of complete β phase solidification path along L \rightarrow L+ $\beta\rightarrow\beta$. Generally, the primary β phase exhibits dendritic morphology during β solidification. For TiAl-based alloys, partition coefficient $k_{\beta/\gamma}$ for Al is less than 1.0 but the β stabilizers (Nb and W) have a partition coefficient higher than 1.0 at β solidification stage^[32,33]. Thus, the dendritic arm (primary β grain) is rich in Nb and W, but Al is rejected to the interdendritic region. In the present study, dendritic core region and dendritic morphology of primary β phase are much less pronounced. The reason can be concluded as the subsequent transformation $\beta\rightarrow\alpha$ together with element diffusion. On the one hand, the transformation $\beta\rightarrow\alpha$ takes place by regarding the Burgers orientation relationship $\{110\}_{\beta}/\{(0001)_{\alpha}$ and $\langle 111 \rangle_{\beta}/\langle 11 \bar{2} 0 \rangle_{\alpha}$, and twelve variants of α with different orientations form in the β grain^[34,35]. On the other hand, composition redistribution takes place during $\beta\rightarrow\alpha$ transformation, and Al diffuses to α phase as the transformation proceeds. But Nb and W diffuse in the opposite direction because the partition coefficient $k_{\beta/\alpha}$ for the β stabilizers (Nb and W) has a value over 1.0^[36]. In this case, the α grain boundaries are rich in Nb and W but poor in Al. Due to the high cooling rate under industrial conditions and β stabilizer addition, the last residual β can be retained at places where α grains meet. Subsequent cooling leads to precipitation of γ phase from α phase according the Blackburn orientation relationship $(0001)_{\alpha}/\{111\}_{\gamma}$ and $\langle 11 \bar{2} 0 \rangle_{\alpha}/\langle 110 \rangle_{\gamma}$, forming lamellar colonies^[1]. Consequently, the retained β phase often segregates along the colony boundaries (prior α grain boundaries). Additionally, suppose that the diffusion of β stabilizers is insufficient somewhere in dendritic core of primary β phase, which can cause some Nb and W enriched

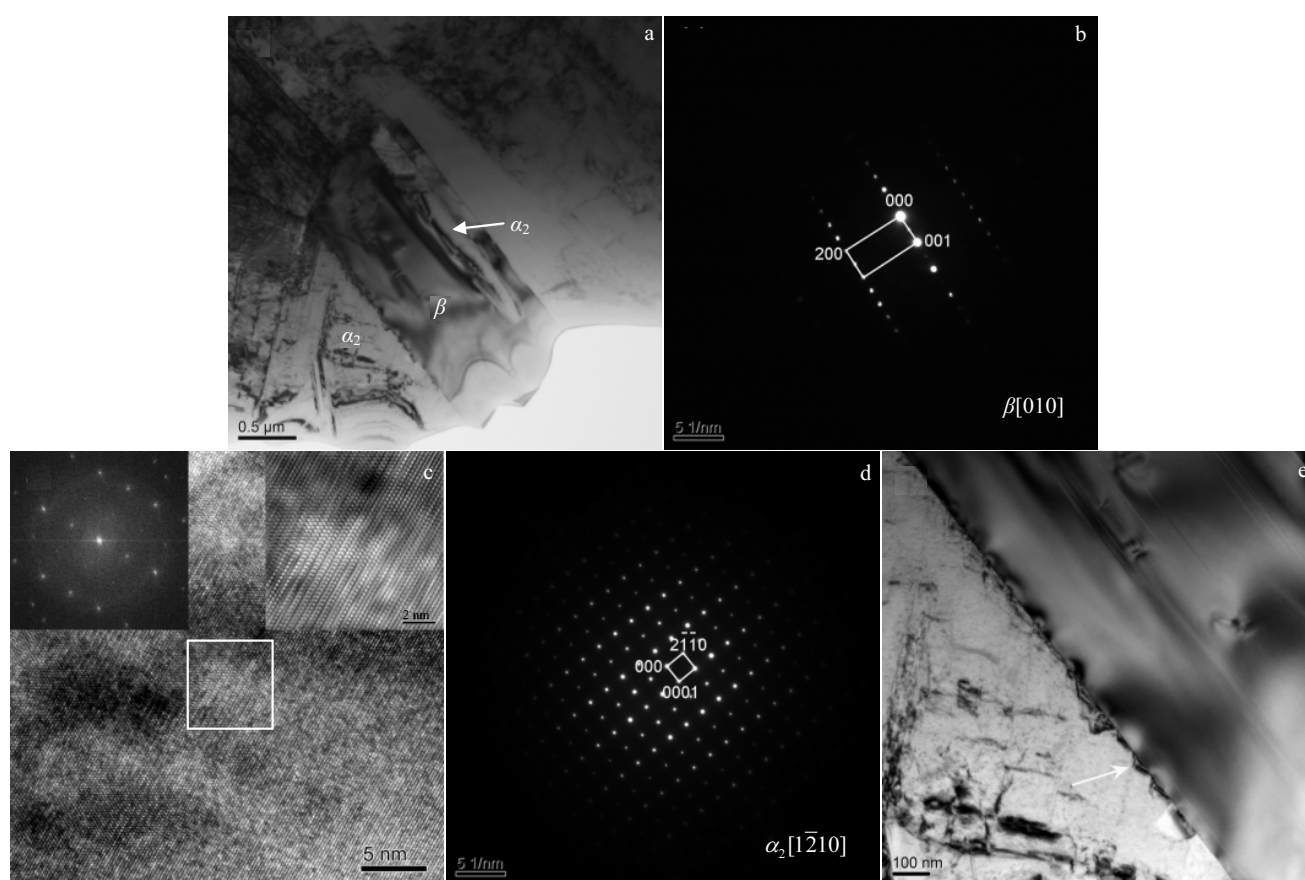


Fig.7 TEM images and SAED patterns of Ti-45Al-8.5Nb-(W, B, Y) alloy deformed at 1200 °C/0.001 s⁻¹: (a) thin secondary α_2 laths forming within a prior β grain, (b) SAED pattern of the β grain, (c) HRTEM image of the secondary α_2 lath together with the corresponding FFT (left inset) and higher magnification (right inset) of the center area marked by rectangle obtained from FFT/IFFT transformation; (d) SAED pattern of surrounding α_2 phase; (e) interface between β grain and surrounding α_2

regions in the lamellar colonies as shown in Fig.2. But the degree of the regions enriched in Nb and W is a little weak, exhibiting a faint outline. The mixture of β /B2 and γ grains has been reported elsewhere^[24,26], formed via $\beta \rightarrow \beta + \gamma$ reaction. In a word, the actual solidification and transformation pathway can be expressed as: $L \rightarrow L + \beta \rightarrow \beta \rightarrow \alpha + \beta \rightarrow \alpha + \text{residual } \beta + \gamma \rightarrow \text{lamellar} + \text{B2} + \gamma$.

3.2 Effect of hot deformation on β /B2 phase evolution

The effect of β phase on the hot deformation have been investigated in literatures^[20,31], while the β /B2 phase can also be influenced by hot-working operations. The β phase is stabilized by β -stabilizers addition expected to exhibit sluggish dissolution behavior because the β -stabilizing elements have such slow diffusion rate^[19,36,37]. However, the diffusion of such slow-diffusing elements can be improved by heat-treatments with applying external pressure^[25]. Considering the short time during hot compression, the variation of the composition of β /B2 phase in this study is related to the high press and temperature. The as-cast lamellar structure is broken up by hot deformation and the

recrystallized grains appear at grain boundaries with increasing temperature. The variation of microstructures must be accompanied with elements diffusion. At the same time, the β /B2 phase is prone to be broken down into fine equiaxed particles, and the distortion and stored energy induced by deformation exist in the β /B2 phase. With decreasing strain rate, the β /B2 phase tends to be spheroidized. The size of β /B2 phase under deformation condition is smaller than that in the as-cast state. It indicates that the contact area between β /B2 phase and other phase is enlarged, and the distance for element diffusion is shortened. It is beneficial for the elements diffusion, including Al atom and β stabilizers. In addition, the diffusion rate of Nb and W is improved because of the sufficient energy provided by the press and increasing temperature. At 1200 °C, the contents of Nb and W in β /B2 phase drop to a relatively low level, which can decrease the stability of β /B2 phase.

When deformed at 1200 °C, transformation β /B2 $\rightarrow\alpha_2$ takes place in the present study. The transformation can proceed via secondary α_2 lath formation in the β /B2 grain, while the β /B2

phase can also be consumed by the neighboring α_2 grains, as shown in Fig.6 and Fig.7. It has been reported that the β phase can transform to α or γ phases after water quenching from the $(\alpha+\beta)$ phase field^[35]. The effect of hot deformation on the $\beta/\text{B2}$ phase is evident, for the transformation can take place at low temperature of the $(\alpha+\gamma)$ phase region. The driving force for the transformation $\beta/\text{B2} \rightarrow \alpha_2$ can be the differences in the densities of atomic packing. The $\beta/\text{B2}$ phase shows bcc crystal structure while the α_2 phase with ordered hexagonal D0_{19} structure exhibits more close-packed arrangement. The transformation most likely takes place by following the Burgers orientation relationship^[35]. Note that the $\{0001\}_{\alpha_2}$ and $\{110\}_{\beta}$ planes are the close-packed planes for α_2 phase and $\beta/\text{B2}$ phase, respectively. And the $\{0001\}$ plane of α_2 phase exhibits hexagonal close-packed structure. Under the deformation condition, the $\beta/\text{B2}$ phase shows a tendency to transform to a more closed packed structure. Additionally, investigations of Xu et al.^[8,16] and Lin et al.^[28] have shown that the $\beta/\text{B2}$ phase in the as-cast TiAl alloy with a similar composition can be eliminated after canned forging in $(\alpha + \gamma)$ phase region.

4 Conclusions

1) As-cast Ti-45Al-8.5Nb-(W, B, Y) alloy exhibits near lamellar (NL) structure with a colony size of about 120 μm , and some segregations exist in the as-cast material as well.

2) The $\beta/\text{B2}$ phase rich in Ti, Nb and W but poor in Al segregates mainly along colony boundaries and triple junctions, and it presents an irregular-shaped block morphology. In addition, some regions slightly enriched in Nb and W exhibits a faint outline, located in the lamellar colonies. These segregations are formed due to the high cooling rate and β stabilizers addition. Besides the microsegregation mentioned above, B-segregation and Y-segregation exist mainly as borides and Y_2O_3 , respectively.

3) Hot deformation has a significant effect on $\beta/\text{B2}$ phase and borides. The $\beta/\text{B2}$ phase is elongated and the long boride rods are broken off after hot deformation. Small cavities are found at the matrix/boride interface after deformed at 850 $^{\circ}\text{C}$, but they disappear when deformed at higher temperature. With increasing temperature, the $\beta/\text{B2}$ phase is prone to broken down into the smaller sized ones. The colonies are surrounded by $\beta/\text{B2}$ phase which is spheroidize when the deformation rate is slow. For the $\beta/\text{B2}$ phase, the Al-content increases while Nb and W contents decrease in the deformed samples, which can reduce the stability of $\beta/\text{B2}$ phase.

4) When the temperature is up to $(\alpha + \gamma)$ phase region, transformation $\beta/\text{B2} \rightarrow \alpha_2$ takes place and it is promoted by hot deformation.

References

- Clemens H, Mayer S. *Adv Eng Mater*[J], 2013, 15: 191
- Loria E A. *Intermetallics*[J], 2000, 8: 1339
- Zhu H, Wei T, Carr D R et al. *JOM*[J], 2012, 64: 1418
- Kim Y W. *JOM*[J], 1994, 46: 30
- Wu X. *Intermetallics*[J], 2006, 14: 1114
- Shu S, Qiu F, Tong C et al. *J Alloy Compd*[J], 2014, 617: 302
- Oehring M, Stark A, Paul J D H et al. *Intermetallics*[J], 2013, 32: 12
- Xu X J, Lin J P, Wang Y L et al. *J Alloy Compd*[J], 2006, 414: 175
- Appel F, Paul J D H, Oehring M. *Gamma Titanium Aluminides-Science and Technology*[M]. Weinheim: Wiley VCH, 2011: 469
- Kothari K, Radhakrishnan R, Wereley N M. *Prog Aerosp Sci*[J], 2012, 55: 1
- Gossler D, Günther R, Hecht U et al. *Acta Mater*[J], 2010, 58: 6744
- Hecht U, Witusiewicz V, Drevermann A et al. *Intermetallics*[J], 2008, 16: 969
- Chen Y Y, Li B H, Kong F T. *J Alloy Compd*[J], 2008, 457: 265
- Kong F T, Chen Y Y, Li B H. *Mater Sci Eng A*[J], 2009, 499: 53
- Chen G L, Xu X J, Teng Z K et al. *Intermetallics*[J], 2007, 15: 625
- Xu X J, Lin J P, Teng Z K et al. *Mater Lett*[J], 2007, 61: 369
- Huang Z W. *Scripta Mater*[J], 2005, 52: 1021
- Sun H L, Huang Z W, Zhu D G et al. *J Alloy Compd*[J], 2013, 552: 213
- Clemens H, Wallgram W, Kremmer S et al. *Adv Eng Mater*[J], 2008, 10: 707
- Tetsui T, Shindo K, Kaji S et al. *Intermetallics*[J], 2005, 13: 971
- Xu X J, Lin J P, Wang Y L et al. *J Alloy Compd*[J], 2006, 414: 131
- Huang L, Liaw P K, Liu C T et al. *Trans Nonferrous Met Soc China*[J], 2011, 21: 2192
- Seo D Y, Beddoes J, Zhao L et al. *Mater Sci Eng A*[J], 2002, 329-331: 810
- Clemens H, Chladil H F, Wallgram W et al. *Intermetallics*[J], 2008, 16: 827
- Zhang D, Dehm G, Clemens H. *Scripta Mater*[J], 2000, 42: 1065
- Zhang Z, Leonard K J, Dimiduk D M et al. In: Hemke K J, Dimiduk D M, Clemens H eds. *Structural Intermetallics 2001*[C]. Warrendale, PA: The Minerals, Metals and Materials Society, 2001: 515
- Hyman M E, McCullough C, Levi, R C G. *Metall Trans A*[J], 1991, 22: 1647
- Lin J P, Xu X.J, Wang Y L et al. *Intermetallics*[J], 2007, 15: 668
- Liu Z C, Lin J P, Wang Y L et al. *Mater Lett*[J], 2004, 58: 948
- Schwaighofer E, Clemens H, Lindemann J et al. *Mater Sci Eng A*[J], 2014, 614: 297
- Liu B, Liu Y, Li Y P et al. *Intermetallics*[J], 2011, 19: 1184
- Klimová A, Lapin J, Tanger L T D. *21st International Conference on Metallurgy and Materials*[C]. Brno: Brno University of Technology, 2012: 1498
- Daloz D, Hecht U, Zollinger J et al. *Intermetallics*[J], 2011, 19:

749

- 34 Jin Y, Wang J N, Yang J et al. *Scripta Mater*[J], 2004, 51: 113
- 35 Cheng T T, Loretto M H. *Acta Mater*[J], 1998, 46: 4801
- 36 Kainuma R, Fujita Y, Mitsui H et al. *Intermetallics*[J], 2000, 8: 855
- 37 Ebrahimi F, Ruiz-Aparicio J G L. *J Alloy Compd*[J], 1996, 245: 1

高 Nb-TiAl 热变形过程中的晶界特征和显微组织演化

赵瑞峰, 周 欢, 张铁邦, 寇宏超, 李金山

(西北工业大学 凝固技术国家重点实验室, 陕西 西安 710072)

摘 要: 研究了 Ti-45Al-8.5Nb-(W,B,Y)合金热变形过程中的晶界特征和显微组织演化规律。采用等离子冷床炉熔炼制备的 Ti-45Al-8.5Nb-(W,B,Y)合金具有典型的近片层组织并在晶界有高温 $\beta/\text{B2}$ 相残留, 富 Nb、W、Ti 等、贫 Al 的晶界 $\beta/\text{B2}$ 相主要是冷床炉熔炼过程中因冷速过快、 β 稳定元素的低扩散系数以及合金中各元素的分配系数差异导致 $\beta \rightarrow \alpha$ 相变不能完全发生。合金中的 B 和 Y 等微量元素分别以硼化物和 Y_2O_3 的形式存在。晶界 $\beta/\text{B2}$ 相的形态、尺寸、成分和稳定性等受后续热变形影响显著, 高温和应力作用会使 β 相发生破碎, 细化并促进合金中的元素扩散会引起晶界 $\beta/\text{B2}$ 相的成分变化。当合金在 $(\alpha+\gamma)$ 两相区进行热压缩变形时, 会有部分 β 相向 α 相转变($\beta/\text{B2} \rightarrow \alpha_2$), 主要通过 β 相中二次 α 的析出和 β 相被相邻 α 相的蚕食等方式进行, 热压缩变形会促进 $\beta/\text{B2}$ 相向更为密排结构的 α_2 相转变。

关键词: TiAl; 晶界特征; 显微组织演化; 微观偏析; 热变形

作者简介: 赵瑞峰, 男, 1976 年生, 博士生, 西北工业大学凝固技术国家重点实验室, 陕西 西安 710072 电话: 029-88491074, E-mail: chinazrf@126.com